Pergamon

Int. J. Solids Structures Vol. 35, Nos 31–32, pp. 4133–4145, 1998

0020–7683/98 $19.00 + .00

PII: S0020–7683(97)00306–5

NONLOCAL MODELS FOR DAMAGE AND FRACTURE: COMPARISON OF APPROACHES

MILAN JIRÁSEK*

Laboratory of Structural and Continuum Mechanics, Department of Civil Engineering, Swiss Federal Institute of Technology (EPFL), CH-1015 Lausanne, Switzerland

(*Received* 15 *November* 1996; *in revised form* 16 *April* 1997)

Abstract—The paper analyzes nonlocal constitutive models used in simulations of damage and fracture processes of quasibrittle materials. A number of nonlocal formulations found in the literature are classified according to the type of variable subjected to nonlocal averaging. Analytical and numerical solutions of a simple one-dimensional localization problem are presented. It is shown that some of the formulations inevitably lead to residual stresses even at very late stages of the deformation process and, consequently, they are not capable of modeling complete separation in a widely open macroscopic crack. The mechanisms leading to this specific type of stress locking are explained based on a theoretical analysis of the nonlocal constitutive equations. It is also pointed out that the nonlocal approach distorts the shape of the stress–strain diagram, which has to be taken into account when designing an appropriate local softening law.

1. INTRODUCTION

As is now widely accepted, standard local constitutive models are inappropriate for materials that exhibit strong strain softening. When the material tangent stiffness matrix ceases to be positive definite, the governing differential equations may lose ellipticity, which renders the boundary value problem ill posed. From the numerical point of view, this situation manifests itself by spurious mesh sensitivity of finite element computations—strain localizes into a narrow band whose width depends on the element size and tends to zero as the mesh is refined. The corresponding load–displacement diagram always exhibits snapback for a sufficiently fine mesh, and the total energy dissipated by fracture converges to zero.

The simplest but crude remedy, popular in engineering applications, is to adjust the post-peak slope of the stress–strain diagram as a function of the element size. When this is done properly, the energy dissipated in a band of cracking elements does not depend on the width of the band. More refined techniques ensuring objectivity are the so-called localization limiters, which include e.g. higher-order gradient models (Aifantis, 1984; Schreyer and Chen, 1986; Vardoulakis and Aifantis, 1991; de Borst and Mühlhaus, 1992; Pamin, 1994), Cosserat continuum (Mühlhaus and Vardoulakis, 1987; de Borst, 1991; Steinmann and Willam, 1992), or viscoplastic regularization (Needleman, 1987).

A computationally efficient and theoretically sound localization limiter is provided by the concept of nonlocal averaging, which is in principle applicable to any type of constitutive model. The idea of a nonlocal continuum originally appeared in elasticity (Eringen, 1966; Kröner, 1968). Its early extensions to strain-softening materials, leading to the so-called imbricate continuum (Bažant, 1984), were later improved by Pijaudier-Cabot and Bažant (1987) who developed a nonlocal damage theory. Bažant and Lin proposed a nonlocal version of a smeared (rotating or fixed) crack model (1988a) and of a model with softening plasticity (1988b), and Bažant and Ožbolt (1990) elaborated a nonlocal microplane model. Localization properties of the nonlocal damage model were extensively studied by Pijaudier-Cabot and Benallal (1993). Saouridis and Mazars (1992) adapted the model for concrete, taking into account the difference between the behaviour in tension and in compression.

* Tel.: 41-21-6932413. Fax: 41-21-6936340. E-mail: milan@lscsun5.epfl.ch.

Finite element implementation of nonlocal plasticity was recently improved by Strömberg and Ristinmaa (1996).

The present paper addresses certain fundamental aspects of nonlocal models. A number of nonlocal formulations found in the literature will be scrutinized, with special attention to proper representation of the entire damage process up to complete failure. Attention will be focused on damage-type models, which unload to the origin. Their behaviour will be illustrated by simple one-dimensional examples.

2. BASIC TYPES OF NONLOCAL FORMULATIONS

2.1. *Concept of nonlocal averaging*

Generally speaking, the nonlocal approach consists in replacing a certain variable by its nonlocal counterpart obtained by weighted averaging over a spatial neighborhood of each point under consideration. If $f(\mathbf{x})$ is some "local" field in a domain V, the corresponding nonlocal field is defined by

$$\bar{f}(\boldsymbol{x}) = \int_V \alpha'(\boldsymbol{x}, \boldsymbol{\xi}) f(\boldsymbol{\xi}) \, \mathrm{d}\boldsymbol{\xi} \tag{1}$$

where $\alpha'(\boldsymbol{x}, \boldsymbol{\xi})$ is a given nonlocal weight function. In an infinite specimen, the weight function depends only on the distance between the "source" point, $\boldsymbol{\xi}$, and the "effect" point, $\boldsymbol{x}$. In the vicinity of a boundary, the weight function is usually rescaled such that the nonlocal operator does not alter a uniform field. This can be achieved by setting

$$\alpha'(\boldsymbol{x}, \boldsymbol{\xi}) = \frac{\alpha(|\boldsymbol{x} - \boldsymbol{\xi}|)}{\int_V \alpha(|\boldsymbol{x} - \boldsymbol{\zeta}|) \, \mathrm{d}\boldsymbol{\zeta}} \tag{2}$$

where $\alpha(r)$ is a monotonically decreasing nonnegative function of the distance $r = |\boldsymbol{x} - \boldsymbol{\xi}|$.

Bažant (1994) suggested to replace the traditional averaging operator (1) by a more complicated implicit scheme, which takes into account not only the distance between $\boldsymbol{x}$ and $\boldsymbol{\xi}$ but also the orientation of principal axes at these points. Ožbolt and Bažant (1996) reported that this modification leads to an improved performance of the nonlocal microplane model, however, the numerical implementation seems to be still under development. It also remains to be verified whether the additional numerical work really pays off for other models as well. In the present study we restrict our attention to standard nonlocal averaging (1).

The weight function is often taken as the Gauss distribution function

$$\alpha(r) = \exp\left(-\frac{r^2}{2l^2}\right) \tag{3}$$

where l is called the internal length of the nonlocal continuum. Another possible choice is the bell-shaped function

$$\alpha(r) = \begin{cases} \left(1 - \dfrac{r^2}{R^2}\right)^2 & \text{if} \quad 0 \leqslant r \leqslant R \\ 0 & \text{if} \quad R \leqslant r \end{cases} \tag{4}$$

where R is a parameter related (but not equal) to the internal length. As R corresponds to the largest distance of point $\boldsymbol{\xi}$ that affects the nonlocal average at point $\boldsymbol{x}$ we suggest to call it the interaction radius. For the Gauss function (3) the interaction radius is $R = \infty$. We also say that function (3) has an unbounded support while function (4) has a bounded support.

From a purely numerical point of view, the choice of the variable to be averaged remains to some extent arbitrary, provided that a few basic requirements are satisfied. First of all, we want the generalized model to exactly agree with the standard local elastic continuum as long as the material behaviour remains in the elastic range. For this reason, it is not possible to simply replace the local strain by nonlocal strain and apply the usual constitutive law. Except for the case of homogeneous strain, nonlocal strain differs from the local one and the model behaviour would be altered already in the elastic range. Second, the model should give a realistic response in simple loading situations such as uniaxial tension. This aspect will be studied in the present paper.

2.2. *Formulations motivated by isotropic damage*

A number of nonlocal concepts giving local response in the linear elastic range have been proposed in the literature. We will illustrate some of them using a simple isotropic damage model (e.g., Lemaitre and Chaboche, 1990). The underlying state equations and evolution law for the local version of the model can be consistently constructed by the standard thermodynamic approach. For numerical implementation, it is advantageous to introduce simple formal modifications (that correspond to closed-form integration of the evolution law), leading to the following set of equations:

$$\boldsymbol{\sigma} = (1-\omega)\boldsymbol{D}_e\boldsymbol{\varepsilon} \tag{5}$$

$$\omega = g(Y_{\max}) \tag{6}$$

$$Y_{\max}(t) = \max_{\tau \leqslant t} Y(\tau) \tag{7}$$

$$Y = \tfrac{1}{2}\boldsymbol{\varepsilon}^{\mathrm{T}}\boldsymbol{D}_e\boldsymbol{\varepsilon} \tag{8}$$

In the above, $\boldsymbol{\sigma}$ is the stress, ε is the strain, $\boldsymbol{D}_e$ is the elastic material stiffness matrix, and ω is the damage parameter that grows from zero (virgin state) to one (fully damaged state) depending on the maximum previously reached value $Y_{\max}$ of the damage energy release rate Y. Of course, Y is not a rate in the sense of a derivative with respect to time. It equals minus the derivative of the free energy $\psi = (1-\omega)\boldsymbol{\varepsilon}^{\mathrm{T}}\boldsymbol{D}_e\boldsymbol{\varepsilon}/2$ with respect to the damage parameter, and so it represents the "rate" at which energy is released as the damage parameter increases (at constant strain and temperature). Function g in (6) controls the evolution of damage and thus affects the shape of the stress–strain curve. It is usually designed such that $\omega = 0$ for $Y_{\max}$ below a certain threshold value, Y_0.

Now, several nonlocal versions of the model can be constructed:

(1) The model originally proposed by Pijaudier-Cabot and Bažant (1987) averages the damage energy release rate Y computed from (8) and evaluates the damage parameter corresponding to the maximum previously reached nonlocal value $\bar{Y}_{\max}$. As long as $Y \leqslant Y_0$ at every point, $\bar{Y}_{\max}$ is also below the threshold and the response is linear elastic.
(2) Bažant and Pijaudier-Cabot (1988) suggested that alternatively one could average the damage parameter ω computed from (6) and substitute its nonlocal value into (5). As long as the material remains (everywhere) elastic, ω is equal to zero and so its nonlocal average is also zero. Equation (5) then reduces to the law of linear elasticity.
(3) The smeared crack model of Bažant and Lin (1988a) dealt with nonlocal strain. Of course, we cannot substitute the averaged strain into (5) because then the model would be nonlocal already in the elastic range. However, if we use the nonlocal strain only in (8) when computing Y and keep the strain in (5) as local then the local character of the initial linear elastic response is preserved.

Table 1. Overview of nonlocal formulations

Formulation	Isotropic damage model	General model
$\omega(\bar{\varepsilon})$	$\boldsymbol{\sigma} = [1-\omega(Y(\bar{\boldsymbol{\varepsilon}}))]\boldsymbol{D}_e\boldsymbol{\varepsilon}$	$\boldsymbol{\sigma} = \boldsymbol{D}_s(\bar{\boldsymbol{\varepsilon}})\boldsymbol{\varepsilon}$
$\bar{Y}$	$\boldsymbol{\sigma} = [1-\omega(\overline{Y(\boldsymbol{\varepsilon})})]\boldsymbol{D}_e\boldsymbol{\varepsilon}$	$\boldsymbol{\sigma} = \boldsymbol{D}_s(\boldsymbol{\Omega}(\overline{\boldsymbol{Y}(\boldsymbol{\varepsilon})}))\boldsymbol{\varepsilon}$
$\bar{\omega}$	$\boldsymbol{\sigma} = [1-\overline{\omega(Y(\boldsymbol{\varepsilon}))}]\boldsymbol{D}_e\boldsymbol{\varepsilon}$	$\boldsymbol{\sigma} = \overline{\boldsymbol{D}_s}(\boldsymbol{\varepsilon})\boldsymbol{\varepsilon}$
$\bar{\gamma}$	$\boldsymbol{\sigma} = [1+\overline{\gamma(Y(\boldsymbol{\varepsilon}))}]^{-1}\boldsymbol{D}_e\boldsymbol{\varepsilon}$	$\boldsymbol{\sigma} = [\boldsymbol{C}_e+\overline{\boldsymbol{C}_i(\boldsymbol{\varepsilon})}]^{-1}\boldsymbol{\varepsilon}$
$\bar{s}$	$\boldsymbol{\sigma} = \boldsymbol{D}_e\boldsymbol{\varepsilon}-\overline{\omega(\boldsymbol{\varepsilon})\boldsymbol{D}_e\boldsymbol{\varepsilon}}$	$\boldsymbol{\sigma} = \boldsymbol{D}_e\boldsymbol{\varepsilon}-\overline{s(\boldsymbol{\varepsilon})}$
$\overline{\Delta s}$	$\dot{\boldsymbol{\sigma}} = (1-\omega)\boldsymbol{D}_e\dot{\boldsymbol{\varepsilon}}-\overline{\dot{\omega}\boldsymbol{D}_e\boldsymbol{\varepsilon}}$	$\dot{\boldsymbol{\sigma}} = \boldsymbol{D}_u\dot{\boldsymbol{\varepsilon}}-\overline{\dot{s}(\boldsymbol{\varepsilon},\dot{\boldsymbol{\varepsilon}})}$
$s(\bar{\varepsilon})$	$\boldsymbol{\sigma} = \boldsymbol{D}_e\boldsymbol{\varepsilon}-\omega(\bar{\boldsymbol{\varepsilon}})\boldsymbol{D}_e\bar{\boldsymbol{\varepsilon}}$	$\boldsymbol{\sigma} = \boldsymbol{D}_e\boldsymbol{\varepsilon}-s(\bar{\boldsymbol{\varepsilon}})$

(4) Pijaudier-Cabot and Bažant (1987) also mentioned that a nonlocal model could be obtained by averaging of the specific fracturing strain. Applying this idea to the isotropic damage law we rewrite (5) as

$$\boldsymbol{\varepsilon} = (1+\gamma)\boldsymbol{C}_e\boldsymbol{\sigma} \tag{9}$$

where $\boldsymbol{C}_e = \boldsymbol{D}_e^{-1}$ is the elastic material compliance matrix and $\gamma = \omega/(1-\omega)$ is the specific fracturing strain. Replacing γ by its weighted average, $\bar{\gamma}$, we construct a nonlocal version of the isotropic damage model.

The above nonlocal formulations are summarized in the upper section of Table 1. For easy reference, we will denote them by symbols $\bar{Y}$, $\bar{\omega}$, etc.; see the first column of Table 1. These formulations were motivated by the isotropic damage model but they can be extended to the class of constitutive laws that express the stress $\boldsymbol{\sigma} = \boldsymbol{D}_s\boldsymbol{\varepsilon}$ as the product of a secant (damaged) stiffness and the strain. The generalized forms are shown in the last column of Table 1. For example, for formulation $\omega(\bar{\varepsilon})$ we use the nonlocal strain as input for the evaluation of the secant stiffness while for formulation $\bar{\omega}$ we first evaluate the secant stiffness locally and then compute its nonlocal average. A natural extension of formulation $\bar{\gamma}$ to the anisotropic case is a model that averages the inelastic compliance, $\boldsymbol{C}_i$.

Anisotropic damage models usually work with a certain damage tensor $\boldsymbol{\Omega}$. A natural extension of formulation $\bar{Y}$ is a model applying nonlocal averaging to the tensor $\boldsymbol{Y}$ that is work-conjugate with $\boldsymbol{\Omega}$.

2.3. *General formulations*

In addition to nonlocal formulations motivated by the isotropic damage model it is possible to develop nonlocal models written directly in a general format.

(5) The elastic response remains local if we average a quantity that is in the elastic state equal to zero, e.g., the inelastic strain. This concept applies to any type of constitutive law formally written as

$$\boldsymbol{\sigma} = \boldsymbol{D}_e(\boldsymbol{\varepsilon}-\boldsymbol{e}) \tag{10}$$

where $\boldsymbol{e}$ is the inelastic strain (fracturing strain, plastic strain, etc.). A nonlocal version of the law is obtained when we replace the inelastic strain by its nonlocal counterpart. If the elastic moduli are uniform throughout the body, this is fully equivalent to a model averaging the inelastic stress

$$\boldsymbol{s} = \boldsymbol{D}_e\boldsymbol{e} = \boldsymbol{D}_e\boldsymbol{\varepsilon}-\boldsymbol{\sigma} \tag{11}$$

The nonlocal law then reads

$$\boldsymbol{\sigma} = \boldsymbol{D}_e \boldsymbol{\varepsilon} - \bar{\boldsymbol{s}} \tag{12}$$

This is the standard version of the generalized nonlocal concept due to Bažant (1994). Note that Bažant worked with the inelastic stress rate

$$\dot{\boldsymbol{s}} = \boldsymbol{D}_e \dot{\boldsymbol{\varepsilon}} - \dot{\boldsymbol{\sigma}} \tag{13}$$

which can be integrated to yield (11).

(6) Alternatively, we could define the inelastic stress rate as

$$\dot{\boldsymbol{s}} = \boldsymbol{D}_u \dot{\boldsymbol{\varepsilon}} - \dot{\boldsymbol{\sigma}} \tag{14}$$

This approach has been taken by Jirásek and Bažant (1994). An important difference compared to (13) is that the elastic stress rate is now $\boldsymbol{D}_u\dot{\boldsymbol{\varepsilon}}$ where $\boldsymbol{D}_u$ is the stiffness matrix valid for unloading. For models with degradation of the elastic moduli, $\boldsymbol{D}_u$ varies during the loading process, and $\dot{\boldsymbol{s}}$ defined by (14) is no longer the time derivative of the quantity $\boldsymbol{s}$ defined by (11). Integration of the nonlocal constitutive law

$$\dot{\boldsymbol{\sigma}} = \boldsymbol{D}_u \dot{\boldsymbol{\varepsilon}} - \dot{\bar{\boldsymbol{s}}} \tag{15}$$

then yields a result different from (12).

(7) Finally, Bažant *et al.* (1996) postulated a general nonlocal constitutive law in the form

$$\boldsymbol{\sigma} = \boldsymbol{D}_e \boldsymbol{\varepsilon} - \boldsymbol{s}(\bar{\boldsymbol{\varepsilon}}) \tag{16}$$

where $\boldsymbol{s}(\bar{\boldsymbol{\varepsilon}})$ is the inelastic stress calculated from the nonlocal strain, $\bar{\boldsymbol{\varepsilon}}$. This means that the actual stress is obtained as the sum of an elastic part evaluated from local strain and an inelastic part evaluated from nonlocal strain.

Of course, general nonlocal formulations (5)–(7) can be specialized to the isotropic damage model by substituting $\boldsymbol{s} = \omega \boldsymbol{D}_e \boldsymbol{\varepsilon}$ for the inelastic stress. The resulting stress–strain equations can be found in the lower section of Table 1.

3. SIMPLE FRACTURE TEST

3.1. *Analytical and numerical solutions*

Let us now test the behaviour of individual nonlocal formulations in an elementary localization problem—tensile failure of a straight uniform bar of length L; see Fig. 1. The bar is divided into a finite number of elements with a linear displacement interpolation inside each element and with one Gauss integration point per element.

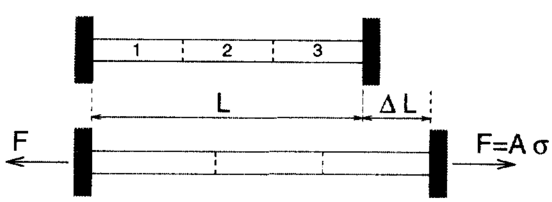

Fig. 1. Bar under uniaxial tension.

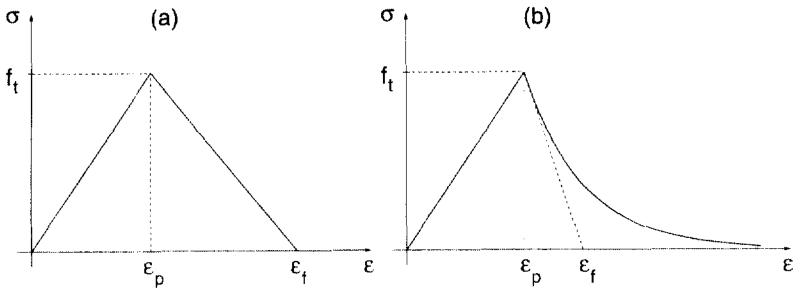

Fig. 2. Local stress–strain law with (a) linear softening, (b) exponential softening.

We will use simple local stress–strain relations with linear elasticity up to the peak stress and either linear or exponential softening; see Fig. 2. The nonlocal formulations will pass the test if, for sufficiently large bar elongations, the residual resistance vanishes and the strain profile keeps its localized character.

Before starting numerical simulations we will study a simple problem solvable by hand. Let us consider a bar divided into three equally sized elements. To render the hand solution feasible we use the local stress–strain relation with linear softening. Of course, such a crude model will not lead to realistic shapes of the load–displacement diagram but it will help us to identify the nature of the problems occurring for some of the formulations.

To facilitate the calculations we fix the parameters of the local constitutive law (Fig. 2(a)) to $f_t = 1$, $\varepsilon_p = 1$, and $\varepsilon_f = 3$, and we consider a bar of cross-sectional area $A = 1$ and length $L = 3$. For linear softening with the chosen parameters, the dependence of the damage parameter on the maximum previously reached strain, $\varepsilon_{\max}$, is given by

$$\omega = \begin{cases} 0 & \text{if} \quad \varepsilon_{\max} \leqslant 1 \\ 1.5\left(1 - \dfrac{1}{\varepsilon_{\max}}\right) & \text{if} \quad 1 \leqslant \varepsilon_{\max} \leqslant 3 \\ 1 & \text{if} \quad 3 \leqslant \varepsilon_{\max} \end{cases} \tag{17}$$

Furthermore, we assume that the interaction radius R from (4) is only slightly larger than the element size and that the discretized nonlocal averaging formulae are

$$\bar{f}_1 = 0.9f_1 + 0.1f_2 \tag{18}$$

$$\bar{f}_2 = 0.1f_1 + 0.8f_2 + 0.1f_3 \tag{19}$$

$$\bar{f}_3 = 0.1f_2 + 0.9f_3 \tag{20}$$

where f_i are local values and $\bar{f}_i$ are nonlocal value of an arbitrary variable f at the centre of element number i. Such an assumption corresponds to slightly different values of R for individual elements ($R_1 = R_3 = 1.2247$, $R_2 = 1.2438$). With this choice, the model response is qualitatively the same as for a uniform interaction radius and the coefficients in the averaging formulae are easy to handle.

- Let us start with formulation $\omega(\bar{\varepsilon})$. At peak stress, $\sigma = f_t = 1$, the load–displacement diagram has a multiple bifurcation point. Besides the uniform solution there exist several solutions with one or two elastically unloading elements. It is possible to show that the steepest descent of the load–displacement diagram is obtained if damage localizes into one of the elements at the boundary while the other two elements unload. Under displacement control, this solution corresponds to the stable branch of the diagram (see Bažant and Cedolin, 1991, Section 10.2).

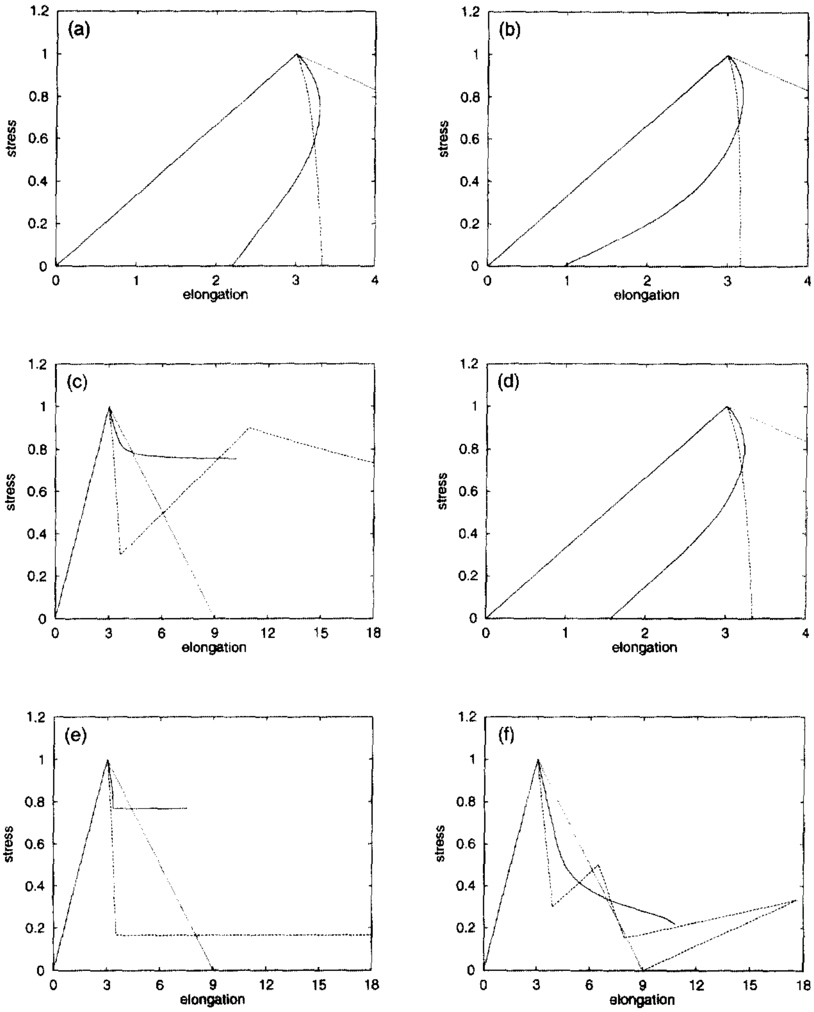

Fig. 3. Load–displacement diagrams for formulation (a) $\omega(\bar{\varepsilon})$, (b) $\bar{Y}$, (c) $\bar{\omega}$, (d) $\bar{\gamma}$, (e) $\overline{\Delta s}$, (f) $\bar{s}$ and $s(\bar{\varepsilon})$. Dashed curves have been obtained with 3 elements, solid curves with 30 elements.

Provided that damage localizes in element number 1, the constitutive law $\sigma = [1-\omega(\bar{\varepsilon})]\varepsilon$ applied at element centres yields

$$\sigma_1 = \left(\frac{1.5}{0.9\varepsilon_1+0.1\varepsilon_2}-0.5\right)\varepsilon_1 \tag{21}$$

$$\sigma_2 = \varepsilon_2 \tag{22}$$

$$\sigma_3 = \varepsilon_3 \tag{23}$$

From equilibrium conditions $\sigma_1 = \sigma_2 = \sigma_3$ we obtain the solution

$$\sigma = \varepsilon_2 = \varepsilon_3 = \sqrt{18.0625\varepsilon_1^2+15\varepsilon_1}-4.75\varepsilon_1 \tag{24}$$

expressed in terms of strain ε_1, which plays the role of a parameter controlling the loading process. The solution remains valid as long as $\bar{\varepsilon}_1 \leqslant 3$. At $\varepsilon_1 = 3.333$ we have $\sigma = \varepsilon_2 = \varepsilon_3 = 0$ and $\bar{\varepsilon}_1 = 3$. The load is fully relaxed and additional increments of applied displacement do not have to oppose any residual resistance. The load–displacement diagram is represented by the dashed curve in Fig. 3(a). The solid curve in the same graph corresponds to a numerical solution with 30 elements while the straight dotted line is the uniform (not localized) solution, i.e., a rescaled local stress–strain curve. The solution with a large number of elements exhibits snapback and the final elongation at complete failure is smaller but the essential feature investigated in the present section is the same as for the solution with three elements—the load is fully relaxed.

- Formulation $\bar{Y}$ leads for the present problem to a quartic equation, which cannot be easily solved by hand. However, the numerically obtained solutions with 3 and 30 elements are very similar to the preceding formulation; see Fig. 3(b).
- The response is substantially different for formulation $\bar{\omega}$. Application of the nonlocal law $\sigma = (1-\bar{\omega})\varepsilon$ at element centres leads to

$$\sigma_1 = 1.35-0.35\varepsilon_1 \tag{25}$$

$$\sigma_2 = \left(0.85+\frac{0.15}{\varepsilon_1}\right)\varepsilon_2 \tag{26}$$

$$\sigma_3 = \varepsilon_3 \tag{27}$$

and from equilibrium we get the solution

$$\varepsilon_2 = \frac{(1.35-0.35\varepsilon_1)\varepsilon_1}{0.85\varepsilon_1+0.15} \tag{28}$$

$$\sigma = \varepsilon_3 = 1.35-0.35\varepsilon_1 \tag{29}$$

These expressions remain valid until $\varepsilon_1 = 3$. At this state, element number 1 is fully *locally* damaged ($\omega_1 = 1$) but the nonlocal damage $\bar{\omega}_1 = 0.9\omega_1+0.1\omega_2 = 0.9 < 1$, and so the element can still transfer stress. Moreover, during the subsequent stage of loading no further damage is produced because ω_1 cannot grow anymore and strains in elements two and three are below the elasticity limit (these elements have been unloaded to strains $\varepsilon_2 = 0.333$ and $\varepsilon_3 = 0.3$). This means that the model responds elastically (with reduced stiffness of elements 1 and 2) until ω_2 starts growing at $\varepsilon_2 = 1$. The load–displacement curve is again rising up to a stress comparable to the tensile strength; see the dashed line in Fig. 3(c). The final stage, during which local damage in element two is growing from 0–1, can be described by

$$\varepsilon_1 = \frac{(1.2-0.3\varepsilon_2)\varepsilon_2}{0.15-0.05\varepsilon_2} \tag{30}$$

$$\varepsilon_3 = \frac{(1.2-0.3\varepsilon_2)\varepsilon_2}{0.15+0.85\varepsilon_2} \tag{31}$$

$$\sigma = 1.2-0.3\varepsilon_2 \tag{32}$$

Surprisingly, as ε_2 approaches 3, ε_1 tends to infinity while σ tends to 0.3. This means that the load–displacement curve asymptotically approaches a horizontal line well above the line of zero stress (this would become obvious if Fig. 3(c) was plotted for a larger range of elongation values). It might be argued that such a paradoxical result is caused by the poor spatial resolution of the model and that the behaviour improves after mesh refinement. A simulation with 30 elements (which is certainly enough to capture all essential features of the solution) gives a monotonically decreasing post-peak curve but again ceases to provide full load relaxation; see the solid curve in Fig. 3(c). Thus, it must be concluded that formulation $\bar{\omega}$ does not meet the fundamental requirement postulated at the beginning of this section. It exhibits a special type of stress locking.

- Formulation $\bar{\gamma}$ leads to full load relaxation and the load–displacement diagram is similar to those produced by formulations $\omega(\bar{\varepsilon})$ and $\bar{Y}$; see Fig. 3(d). The post-peak solution is described by

$$\varepsilon_2 = \frac{(2.7-0.7\varepsilon_1)\varepsilon_1}{0.3+1.3\varepsilon_1} \tag{33}$$

$$\sigma = \varepsilon_3 = \frac{(3-\varepsilon_1)\varepsilon_1}{0.3+1.3\varepsilon_1} \tag{34}$$

An interesting difference compared to formulations $\omega(\bar{\varepsilon})$ and $\bar{Y}$ is that, at complete failure, the strain does not localize into a single element (at $\varepsilon_1 = 3$ we have $\sigma = \varepsilon_3 = 0$ but $\varepsilon_2 = 0.333 \neq 0$).

- The initial post-peak response of the model with nonlocal inelastic stress rate is described by

$$\varepsilon_2 = 1.5-0.5\varepsilon_1+0.3\ln\varepsilon_1 \tag{35}$$

$$\sigma = \varepsilon_3 = 1.5-0.5\varepsilon_1+0.15\ln\varepsilon_1 \tag{36}$$

This corresponds to a reasonable descending branch in the load–displacement diagram; see Fig. 3(e). However, at $\varepsilon_1 = 3$ the stress ceases to decrease and the diagram continues by a horizontal line. The reason is that local inelastic stress increments in all elements are now zero (element one is fully damaged and elements two and three are locally in the elastic range). As the unloading stiffness of element 1 is also zero, no stress change is possible in that element. The same type of behaviour, only with a larger value of the residual stress, is exhibited by the model with 30 elements.

- Finally, for formulation $\bar{s}$ we get a diagram with alternating ascending and descending straight segments; see Fig. 3(f). Each descending segment corresponds to softening in one of the elements while the other elements are locally either in the elastic range or fully damaged. This alternating effect is indeed due to the poor spatial resolution and is not present in the simulation with 30 elements. However, the important point is that independently of the discretization the stress drops down to zero only after all elements have been fully damaged! Consequently, the final strain profile is not localized but uniform. Even though formulations $\bar{s}$ and $s(\bar{\varepsilon})$ are in general different, the corresponding load–displacement diagrams (not the strain profiles) happen to be the same (for the present simple uniaxial problem).

3.2. *Theoretical analysis of locking mechanisms*

The fact that formulation $\bar{s}$ must give a uniform strain profile at complete failure can be proven theoretically without resorting to finite element discretization. At complete failure, the stress at every point is zero, and so the nonlocal constitutive relation (12) combined with (11) and reduced to one dimension gives

$$E\left[\varepsilon(x)-\int_0^L \alpha'(x,\xi)e(\xi)\,d\xi\right] = 0 \tag{37}$$

Young's modulus E is positive, and so the expression in brackets must vanish. This condition can be rewritten as

$$\int_0^L \alpha'(x,\xi)[\varepsilon(x)-e(\xi)]\,d\xi = 0 \tag{38}$$

because the weight function is normalized, $\int_0^L \alpha'(x,\xi)\,d\xi = 1$. Note that (38) must hold for

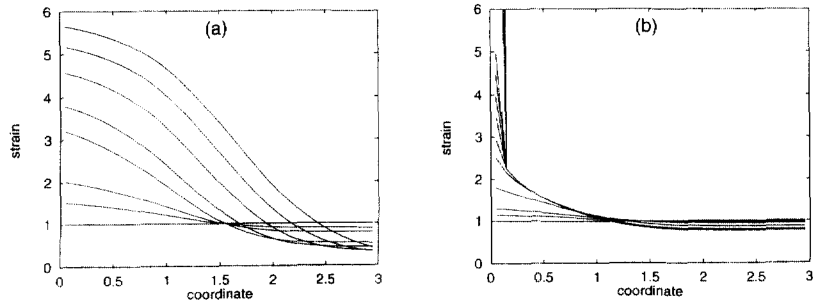

Fig. 4. Evolution of strain profile for formulations (a) $\bar{s}$, (b) $\overline{\Delta s}$.

any x. Let us denote by x_0 the point with the largest strain. The inelastic strain can nowhere exceed $\varepsilon(x_0)$, i.e., $\varepsilon(x_0)-e(\xi) \geqslant 0$ for any ξ. Moreover, $\alpha'(x_0, \xi)$ is nonnegative for any ξ and is strictly positive for $\xi \in (x_0-R, x_0+R)$ where R is the interaction radius. Consequently, (38) can hold at $x = x_0$ only if $\varepsilon(x_0) = e(\xi)$ for any $\xi \in (x_0-R, x_0+R)$. For a weight function with unbounded support this means that $\varepsilon(\xi) = \varepsilon(x_0) = \text{const}$ everywhere. But even if the weight function has a bounded support, we can recursively apply the same argument at x_0 shifted by $\pm nR/2$, $n = 1, 2, \ldots$, and arrive at the conclusion that the strain is constant along the entire bar. This explains why the formulation with nonlocal inelastic stress cannot properly represent localized deformation at complete failure. The progressive expansion of the process zone is documented in Fig. 4(a), which shows the evolution of the strain profile obtained numerically for the test problem analyzed in the preceding subsection.

Similarly, we can explain the stress-locking behaviour of formulation $s(\bar{\varepsilon})$. Analyzing the situation at complete failure when $\sigma = E\varepsilon - s(\bar{\varepsilon}) = 0$ and using the fact that the inelastic stress cannot exceed the elastic stress computed for the same strain, $s(\bar{\varepsilon}) \leqslant E\bar{\varepsilon}$, we can derive an inequality

$$\int_0^L \alpha'(x, \xi)[\varepsilon(x)-\varepsilon(\xi)]\,\mathrm{d}\xi \leqslant 0 \tag{39}$$

that must be satisfied for every $x \in \langle 0, L \rangle$. Again, it can be concluded that the strain profile must be uniform.

Let us now look at the behaviour of formulation $\bar{\omega}$. The constitutive equation in one dimension reads

$$\sigma = (1-\bar{\omega})E\varepsilon \tag{40}$$

where

$$\bar{\omega}(x) = \int_0^L \alpha'(x, \xi)\omega(\xi)\,\mathrm{d}\xi \tag{41}$$

At complete fracture we have $\sigma(x) = 0$ and so there must exist a point x_0 at which

$$\bar{\omega}(x_0) = 1 \tag{42}$$

otherwise the strain would have to vanish identically and the total extension of the bar would be zero. However, as $\omega(\xi) \leqslant 1$ for any ξ, (42) can hold only if $\omega(\xi) = 1$ whenever $\alpha'(x_0, \xi) > 0$. For a weight function with unbounded support this means that every point of the bar must be completely damaged. The rigorous proof of a similar statement for a weight function with bounded support would be more tricky but even in this case the model is incapable of capturing localized damage at complete failure.

We can also explain the mechanism of stress locking for formulation $\overline{\Delta s}$. For a plasticity-type model, in which unloading takes place with the initial stiffness, the formulation is identical with the approach using nonlocal inelastic stress, and the criticism of formulation $\bar{s}$ applies. For a damage-type model with degradation of elastic stiffness, the problem appears as soon as the point x_0 with maximum strain reaches the state of complete local damage. The current unloading modulus E_u at x_0 is now zero and arbitrary strain increments at x_0 do not affect the stress state. Therefore, strain increments fully localize into this single point while the stress remains constant (and different from zero). This behaviour is documented in Fig. 4(b), which shows the evolution of the strain profile obtained numerically for the test problem analyzed in the preceding subsection.

4. CONCLUDING REMARKS

We have shown that certain nonlocal formulations are inherently incapable of reproducing the entire material degradation process up to complete failure. Unless we are interested only in the response at the onset of localization, models that exhibit the special type of stress locking described in the previous section should be avoided. Theoretical analysis of the locking mechanisms revealed that the pathological behaviour must appear independently of the particular value of the internal length or interaction radius.

Let us add a few comments on the formulations that do have the potential of properly describing localized damage up to the formation of a stress-free crack. Formulations $\bar{Y}$ and $\omega(\bar{\varepsilon})$ deal, respectively, with nonlocal damage energy release rate and nonlocal strain, and so they are quite similar because the damage energy release rate can be interpreted as the square of a generalized strain norm. In one dimension we simply have $Y = E\varepsilon^2/2$, which means that formulation $\bar{Y}$ averages the square of strain while formulation $\omega(\bar{\varepsilon})$ averages the strain itself. Numerical experience with simulations of tensile failure indicates that in general there are only minor differences between the results obtained with the two approaches. From computational point of view it is less expensive to average the damage energy release rate because it is a scalar quantity. Also, averaging of energy seems to be somewhat more logical from the physical point of view.

On the other hand, the formulation with nonlocal strain is more general because it can be extended to the class of constitutive laws written in the form $\boldsymbol{\sigma} = \boldsymbol{D}_s(\boldsymbol{\varepsilon})\boldsymbol{\varepsilon}$; see Table 1. In the nonlocal version, we evaluate the unloading (secant) stiffness matrix from the nonlocal strain and then multiply it by the local strain to obtain the actual stress. This concept can be applied for example to the microplane model (Bažant and Ožbolt, 1990) and to the fixed or rotating crack model (Bažant and Lin, 1988a; Jirásek and Zimmermann, 1998).

Alternatively, formulation $\bar{\gamma}$ could be used for the same purpose. Nonlocal averaging would be applied to the inelastic material compliance matrix $\boldsymbol{C}_i$, which requires an even larger amount of computational work than averaging of the strain.

Load–displacement diagrams of concrete specimens tested under direct tension typically exhibit a relatively steep drop immediately after the peak load, followed by a long tail. As is clear from Fig. 3(a, b, d), the shapes of diagrams obtained with a nonlocal model using a linear local softening law are not at all realistic. More reasonable response is produced by an exponential local softening law; see Fig. 5. The total amount of energy dissipated in a uniaxial tensile test is affected mainly by the area under the local stress–strain curve and by the internal length. However, it also exhibits a weak dependence on the shape of the softening curve, type of nonlocal weight function, and type of nonlocal formulation (quantity to be averaged). The parameter identification procedure has therefore an iterative character.

Due to its limited extent, the present study has dealt exclusively with damage-type models that unload to the origin. Another sound nonlocal approach can be developed in the context of plasticity. Comparison of nonlocal damage and plasticity theories and analysis of the structure and evolution of the process zone shall be presented in a separate paper, along with a discussion of the parameter identification procedure.

Finally, it should be admitted that there remain a number of open questions related to the nonlocal theory. The present paper has not paid too much attention to thermodynamic aspects of nonlocal models, nor to the physical interpretation of the averaging

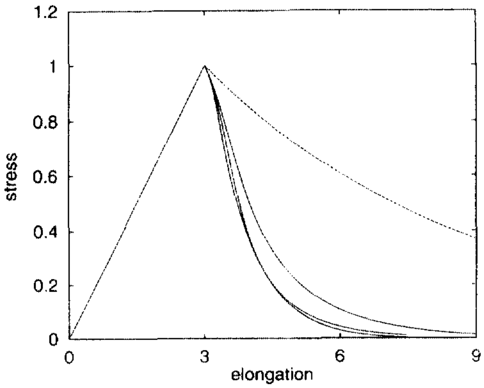

Fig. 5. Load–displacement diagrams for nonlocal formulations using an exponential local law. Dashed curve corresponds to the uniform solution, solid curves are stable paths for formulations $\omega(\bar{\varepsilon})$, $\bar{\gamma}$, and $\bar{Y}$ (from top to bottom).

procedure. The principal aim here was to detect the nonlocal formulations that lead to qualitatively unacceptable response and therefore should be *a priori* excluded from consideration.

Thermodynamic framework was used by Eringen (1981, 1983) in his papers on nonlocal plasticity, which dealt only with the special case when nonlocal strain completely replaces local strain as an argument of the constitutive operator. Recent work by Strömberg and Ristinmaa (1996), Polizzotto *et al.* (1997), and others should eventually lead to the establishment of a consistent and generally accepted thermodynamic basis.

Physical interpretation of nonlocal averaging was addressed by Bažant (1994) and, in a somewhat different context, by Drugan and Willis (1996). However, the effect of boundaries and material interfaces on the averaging operator still remains an open issue, same as the dependence of the internal length on the stress state. Let us hope that micromechanical simulations and sophisticated experimental techniques will provide better insight into the damage processes on the mesoscale and help to resolve some of the outstanding problems.

Acknowledgement—Financial support of the Swiss Committee for Technology and Innovation (CTI) under project CERS.2638.1 is gratefully acknowledged.

REFERENCES

Aifantis, E. C. (1984) On the microstructural origin of certain inelastic models. *Journal of Engineering Materials and Technology, ASME* **106,** 326–330.

Bažant, Z. P. (1984) Imbricate continuum and its variational derivation. *Journal of Engineering Mechanics, ASCE* **110,** 1593–1712.

Bažant, Z. P. (1994) Nonlocal damage theory based on micromechanics of crack interactions. *Journal of Engineering Mechanics, ASCE* **120,** 593–617, with Addendum in **120,** 1401–1402.

Bažant, Z. P. and Cedolin, L. (1991) *Stability of Structures*. Oxford University Press, New York and Oxford.

Bažant, Z. P. and Lin, F.-B. (1988a) Nonlocal smeared cracking model for concrete fracture. *Journal of Engineering Mechanics, ASCE* **114,** 2493–2510.

Bažant, Z. P. and Lin, F.-B. (1988b) Nonlocal yield-limit degradation. *International Journal for Numerical Methods in Engineering* **26,** 1805–1823.

Bažant, Z. P. and Ožbolt, J. (1990) Nonlocal microplane model for fracture, damage, and size effect in structures. *Journal of Engineering Mechanics, ASCE* **116,** 2485–2505.

Bažant, Z. P. and Pijaudier-Cabot, G. (1988) Nonlocal continuum damage, localization instability and convergence. *Journal of Applied Mechanics, ASME* **55,** 287–293.

Bažant, Z. P., Xiang, Y., Adley, M., Prat, P. C. and Akers, S. A. (1996) Microplane model for concrete: II. Data delocalization and verification. *Journal of Engineering Mechanics, ASCE* **122,** 255–262.

de Borst, R. (1991) Simulation of strain localization: a reappraisal of the Cosserat continuum. *Engineering Computations* **8,** 317–332.

de Borst, R. and Mühlhaus, H.-B. (1992) Gradient-dependent plasticity: formulation and algorithmic aspects. *International Journal for Numerical Methods in Engineering* **35,** 521–539.

Drugan, W. J. and Willis, J. R. (1996) A micromechanics-based nonlocal constitutive equation and estimates of representative volume element size for elastic composites. *Journal of the Mechanics and Physics of Solids* **44,** 497–524.

Eringen, A. C. (1966) A unified theory of thermomechanical materials. *International Journal of Engineering Science* **4,** 179–202.

Eringen, A. C. (1981) On nonlocal plasticity. *International Journal of Engineering Science* **19,** 1461–1474.
Eringen, A. C. (1983) Theories of nonlocal plasticity. *International Journal of Engineering Science* **21,** 741–751.
Jirásek, M. and Bažant, Z. P. (1994) Localization analysis of nonlocal model based on crack interactions. *Journal of Engineering Mechanics, ASCE* **120,** 1521–1542.
Jirásek, M. and Zimmermann, T. (1998). Rotating crack model with transition to scalar damage. *Journal of Engineering Mechanics, ASCE* **124,** 277–284.
Kröner, E. (1968) Elasticity theory of materials with long-range cohesive forces. *International Journal of Solids and Structures* **3,** 731–742.
Lemaitre, J. and Chaboche, J.-L. (1990) *Mechanics of Solid Materials*. Cambridge University Press, Cambridge, UK.
Mühlhaus, H.-B. and Vardoulakis, I. (1987) The thickness of shear band in granular materials. *Géotechnique* **37,** 271–283.
Needleman, A. (1987) Material rate dependence and mesh sensitivity in localization problems. *Computer Methods in Applied Mechanics and Engineering* **67,** 68–85.
Ožbolt, J. and Bažant, Z. P. (1966) Numerical smeared fracture analysis: Nonlocal microcrack interaction approach. *International Journal for Numerical Methods in Engineering* **39,** 635–661.
Pamin, J. (1994) Gradient-Dependent Plasticity in Numerical Simulation of Localization Phenomena. Doctoral dissertation, TU Delft, The Netherlands.
Polizzotto, C., Borino, G. and Fuschi, P. (1997) Gradient plasticity—a thermodynamic formulation. In *Computational Plasticity*, ed. D. R. J. Owen, E. Oñate and E. Hinton, pp. 481–488. CIMNE, Barcelona.
Pijaudier-Cabot, G. and Bažant, Z. P. (1987) Nonlocal damage theory. *Journal of Engineering Mechanics, ASCE* **113,** 1512–1533.
Pijaudier-Cabot, G. and Benallal, A. (1993) Strain localization and bifurcation in nonlocal continuum. *International Journal of Solids and Structures* **30,** 1761–1775.
Saouridis, C. and Mazars, J. (1992) Prediction of the failure and size effect in concrete via a bi-scale damage approach. *Engineering Computations* **9,** 329–344.
Schreyer, H. and Chen, Z. (1986) One-dimensional softening with localization. *Journal of Applied Mechanics, ASME* **53,** 791–797.
Steinmann, P. and Willam, K. (1992) Localization within the framework of micropolar elastoplasticity. In *Advances in Continuum Mechanics*, ed. V. Mannl *et al.*, pp. 296–313. Springer Verlag, Berlin.
Strömberg, L. and Ristinmaa, M. (1996) FE-formulation of a nonlocal plasticity theory. *Computer Methods in Applied Mechanics and Engineering* **136,** 127–144.
Vardoulakis, I. and Aifantis, E. C. (1991) A gradient flow theory of plasticity for granular materials. *Acta Mechanica* **87,** 197–217.